

- Breimer, L. H. (1984) *Nucleic Acids Res.* 12, 6359-6367.
- Breimer, L. H., & Lindahl, T. (1980) *Nucleic Acids Res.* 8, 6199-6211.
- Breimer, L. H., & Lindahl, T. (1984) *J. Biol. Chem.* 259, 5543-5548.
- Burton, K., & Riley, W. T. (1966) *Biochem. J.* 98, 70-77.
- Cadet, J., Berger, M., & Voituriez, L. (1982) *J. Chromatogr.* 238, 488-494.
- Cathcart, R., Schwiers, E., Saul, R. L., & Ames, B. N. (1984) *Proc. Natl. Acad. Sci. U.S.A.* 81, 5633-5637.
- Cerutti, P. A. (1976) in *Photochemistry and Photobiology of Nucleic Acids* (Wang, S. Y., Ed.) Vol. II, pp 375-401, Academic Press, New York.
- Cunningham, R. P., & Weiss, B. (1985) *Proc. Natl. Acad. Sci. U.S.A.* 82, 474-478.
- Demple, B., & Linn, S. (1980) *Nature (London)* 287, 203-208.
- Glickman, B. W., Rietveld, K., & Aaron, C. S. (1980) *Mutat. Res.* 69, 1-12.
- Hollstein, M. C., Brooks, P., Linn, S., & Ames, B. N. (1984) *Proc. Natl. Acad. Sci. U.S.A.* 81, 4003-4007.
- Iida, S., & Hayatsu, H. (1970) *Biochim. Biophys. Acta* 213, 1-13.
- Iida, S., & Hayatsu, H. (1971) *Biochim. Biophys. Acta* 218, 1-8.
- Jones, A. S., Ross, G. W., Takemura, S., Thompson, T. W., & Walker, R. T. (1964) *J. Chem. Soc.*, 373-378.
- Katcher, H. L., & Wallace, S. S. (1983) *Biochemistry* 22, 4071-4082.
- Kato, K. I., Goncalves, J. M., Houts, G. E., & Bollum, F. J. (1967) *J. Biol. Chem.* 242, 2780-2789.
- Levin, D. E., Hollstein, M., Christman, M. F., Schwiers, E. A., & Ames, B. N. (1982) *Proc. Natl. Acad. Sci. U.S.A.* 79, 7445-7449.
- Murahashi, S., Yuki, H., Kosai, K., & Doura, F. (1966) *Bull. Chem. Soc. Jpn.* 39, 1559-1562.
- Nofre, C., & Cier, A. (1966) *Bull. Soc. Chim. Fr.*, 1326-1333.
- Rigby, P. W. J., Dieckmann, M., Rhodes, C., & Berg, P. (1977) *J. Mol. Biol.* 113, 237-251.
- Scholes, G. (1976) in *Photochemistry and Photobiology of Nucleic Acids* (Wang, S. Y., Ed.) Vol. I, pp 521-574, Academic Press, New York.
- Swinehart, J. L., Lin, W. S., & Cerutti, P. A. (1974) *Radiat. Res.* 58, 166-175.
- Teebor, G. W., Frenkel, K., & Goldstein, M. S. (1984) *Proc. Natl. Acad. Sci. U.S.A.* 81, 318-321.
- Teoule, R., Bert, C., & Bonicel, A. (1977) *Radiat. Res.* 72, 190-200.
- Teoule, R., Bonicel, A., Bert, C., & Fouque, B. (1978) *J. Am. Chem. Soc.* 100, 6749-6750.

## Change of Conformation and Internal Dynamics of Supercoiled DNA upon Binding of *Escherichia coli* Single-Strand Binding Protein<sup>†</sup>

Jörg Langowski, Albert S. Benight, Bryant S. Fujimoto, and J. Michael Schurr\*

*Department of Chemistry, University of Washington, Seattle, Washington 98195*

Ulrich Schomburg

*Zentrum Biochemie, Abteilung Biophysikalische Chemie, Medizinische Hochschule, D-3000 Hannover 61, Federal Republic of Germany*

*Received October 1, 1984; Revised Manuscript Received February 20, 1985*

**ABSTRACT:** The influence of *Escherichia coli* single-strand binding (SSB) protein on the conformation and internal dynamics of pBR322 and pUC8 supercoiled DNAs has been investigated by using dynamic light scattering at 632.8 and 351.1 nm and time-resolved fluorescence polarization anisotropy of intercalated ethidium. SSB protein binds to both DNAs up to a stoichiometry that is sufficient to almost completely relax the superhelical turns. Upon saturation binding, the translational diffusion coefficients ( $D_0$ ) of both DNAs decrease by approximately 20%. Apparent diffusion coefficients ( $D_{app}$ ) obtained from dynamic light scattering display the well-known increase with  $K^2$  ( $K$  = scattering vector), leveling off toward a plateau value ( $D_{plat}$ ) at high  $K^2$ . For both DNAs, the difference  $D_{plat} - D_0$  increases upon relaxation of supercoils by SSB protein, which indicates a corresponding enhancement of the subunit mobilities in internal motions. Fluorescence polarization anisotropy measurements on free and complexed pBR322 DNA indicate a (predominantly) uniform torsional rigidity for the saturated DNA/SSB protein complex that is significantly reduced compared to the free DNA. These observations are all consistent with the notion that binding of SSB protein is accompanied by a gradual loss of supercoils and saturates when the superhelical twist is largely removed.

It is an established fact that supercoiling can influence the local structure of DNA in a variety of ways. Since the native

superhelical twist of DNA is opposite to the sense of twist of the B-DNA helix, supercoiling generally destabilizes the B helix, making processes that decrease the superhelical density of covalently closed circular DNA chains such as cruciform formation (Lilley, 1980; Panayotatos & Wells, 1981; Mizuuchi et al., 1982; Lilley & Markham, 1983) or B- to Z-helix transition (Pohl & Jovin, 1972; Wang et al., 1979; O'Connor

<sup>†</sup>This work was supported in part by National Institutes of Health Grants R01 GM29338 and R01 GM32302. J.L. is the recipient of Research Fellowship La 500/1-1 from the Deutsche Forschungsgemeinschaft.

et al., 1983; Jovin et al., 1983) more likely to occur. Melting of B-helix turns is another mechanism by which to relax superhelical strain from a plasmid; proteins such as *Escherichia coli* single-strand binding (SSB) protein (Krauss et al., 1981) that bind specifically to single-strand DNA and promote the denaturation of double-strand DNA might be expected to bind to negatively supercoiled DNA.

Indeed, it has been shown recently that SSB protein binds to double-strand supercoiled DNA, thereby altering the global conformation from supercoil to relaxed circular and changing the pattern of S1 cleavage (Glikin et al., 1983). Although those experiments qualitatively established that SSB protein can locally melt supercoiled DNA and bind to it, the purpose of that work was to map the location of the binding sites rather than determining physical parameters of the binding itself. We were interested in how the binding of *E. coli* SSB protein to supercoiled DNA influences the solution structure and the internal dynamics of the DNA. Optical methods such as dynamic light scattering (DLS) and fluorescence polarization anisotropy decay (FPA) serve as powerful tools to gather information about the structural and dynamic properties of DNA and have been applied to monitor solution structure and internal motions in many different systems (Schurr, 1977; Wilcoxon et al., 1982). In this paper, DLS and FPA experiments are described that quantitatively measure changes in the diffusion coefficient and in the internal dynamics of supercoiled plasmid DNA when SSB protein is bound.

#### MATERIALS AND METHODS

***E. coli* Single-Strand Binding (SSB) Protein.** *E. coli* SSB protein is a tetramer with a subunit molecular weight of 20 000 (Krauss et al., 1981). It binds cooperatively to single-strand DNAs but does not bind strongly to linear double-strand DNA. The binding covers approximately 8–10 nucleotides per monomeric subunit, and a single-strand DNA chain can wrap around the tetramer so that 40 nucleotides are bound (Krauss et al., 1981). Values between  $5 \times 10^8 \text{ M}^{-1}$  for the binding constant of a single tetramer to a 40 base pair oligonucleotide (Krauss et al., 1981) and  $10^{10}$ – $10^{11} \text{ M}^{-1}$  for cooperative binding to longer DNA (Ruyechan & Wetmur, 1975) have been reported. The dissociation of the bound protein is slow with a dissociation rate  $< 1 \text{ s}^{-1}$  (Krauss et al., 1981). SSB protein was prepared as described previously (Krauss et al., 1981).

**Plasmid Preparation.** Cultures of *E. coli* strain HB101 harboring plasmid pBR322 or pUC8 were initiated in 250 mL of L broth in the presence of 100  $\mu\text{g}/\text{mL}$  ampicillin and grown overnight at 37 °C. This overnight culture was then added to 1 L of M9 medium (Maniatis et al., 1982) supplemented with 1 mM  $\text{CaCl}_2$ , 10 mM  $\text{MgSO}_4$ , 4 g/L glucose, 5 g/L casamino acids, 4 mg/L thiamin, and 100 mg/L ampicillin and shaken for several hours until the culture turbidity ( $A_{600}$ ) reached 1.2. At this point, the growing culture was transferred into a fermenter jar (New Brunswick Scientific Microferm) containing 10 L of M9 with supplements and ampicillin. Growth continued under forced aeration and stirring at 37 °C until the  $A_{600}$  reached 1.8. At this point, plasmid amplification was effected by adding chloramphenicol to a final concentration of 150 mg/L. Stirring was continued overnight for 16–19 h.

Cell harvest was by centrifugation at 4000  $\text{min}^{-1}$  for 30 min. After the first centrifugation, cell pellets were resuspended and washed in TES buffer [50 mM tris(hydroxymethyl)aminomethane (Tris), 50 mM ethylenediaminetetraacetic acid (EDTA) pH 8.0, and 15% sucrose], repelleted, and stored by freezing at  $-20 \text{ }^\circ\text{C}$ . Typical preparations netted 40 g of wet packed cells.

Cell lysis and separation of plasmid DNA from chromosomal DNA and other cellular debris were by a modification of a technique given in the BRL NACS applications manual (Langowski et al., 1984). Following treatments with 100  $\mu\text{g}/\text{mL}$  RNase and 5  $\mu\text{g}/\text{mL}$  proteinase K, plasmid DNA was precipitated with poly(ethylene glycol) (PEG). PEG pellets were redissolved in buffer, extracted 3 times with phenol and 4 times with ether, and exhaustively dialyzed against 0.1 M NaCl, 10 mM Tris, and 1 mM EDTA, pH 7.2. Covalently closed circular plasmid DNA was separated from other forms and chromosomal fragments by banding twice in CsCl/ethidium equilibrium density gradients. The DNA fractions extracted from gradient lower bands were found to contain >90% monomer covalently closed circular plasmid DNA as determined by electrophoresis in 1% agarose gels.

Alternatively, pUC8 was purified from the PEG pellet by RPC-5 column chromatography as described elsewhere (Langowski et al., 1984). Yield and purity were similar to those for the CsCl-banded samples.

High-purity supercoiled plasmid, deemed protein free from the absorbance ratio  $A_{260}/A_{280} > 2.0$ , was precipitated with 2 volumes of ethanol and redissolved to its final concentration in 0.1 M NaCl, 10 mM Tris, and 1 mM EDTA, pH 7.2 (0.1 TE), buffer that had been prefiltered through a 0.22- $\mu\text{m}$  Millipore filter. Prior to light-scattering experiments, approximately 18 mL of this solution was filtered under gravity flow through a two-stage 0.45- $\mu\text{m}$  Duropore filter cascade into a clean prewashed cylindrical scattering cell.

SSB protein was not filtered prior to addition to the DNA due to the small volume available. As a consequence, small dust particles were introduced into the light-scattering cell together with the protein. However, dust "Tyndalls" were virtually undetectable until the very highest protein concentrations were reached. The influence of dust on the results is therefore considered negligible.

DLS measurements were performed at room temperature (21 °C) on a single DNA sample prepared 4–6 weeks prior to experiments. Titrations of plasmid DNA with SSB protein were performed by adding SSB to the DNA solution. After each protein addition, a scattering curve of the apparent diffusion coefficient ( $D_{\text{app}}$ ) vs.  $K^2$  was obtained over a wide range of  $K^2$  values ( $0.47 \times 10^{10} \text{ cm}^{-2} \leq K^2 \leq 19.2 \times 10^{10} \text{ cm}^{-2}$ ), using 632.8- and 351.1-nm light. Such measurements generally required 7–8 h collection time. Data collection for the whole titration curve extended over a 2-week period. After each day of experiments, the scattering cell containing the DNA/protein solution was stored in the refrigerator at 4 °C. Before the next protein addition, the solution was allowed to warm up to room temperature, and several  $D_{\text{app}}$  vs.  $K^2$  values were measured. These measurements always agreed within experimental error with those taken the previous day, thus ensuring the protein/DNA system had experienced no change in its hydrodynamic properties due to cold storage.  $D_{\text{app}}$  values reported were the average from three correlation functions each.

**Light-Scattering System.** The apparatus for dynamic light scattering was similar to that described previously (Lin et al., 1981). A 50-mW He–Ne laser (Spectra-Physics 125) operating at 632.8 nm and a 100-mW Ar ion laser operating at 351.1 nm served as light sources. Together these lasers provided a range of  $K^2$  values from  $0.47 \times 10^{10}$  to  $19.12 \times 10^{10} \text{ cm}^{-2}$ .

The 248-channel digital photon correlator is a slight modification of that described previously (Thomas & Schurr, 1979; Thomas et al., 1980a,b; Lin et al., 1981). Correlation functions

covering approximately eight decay times were fitted to a single exponential plus base line, and  $D_{app}$  was calculated from the resulting relaxation time ( $\tau$ ) according to the relation  $D_{app} = 1/2\tau K^2$ . An index of refraction  $n = 1.334$  for the  $\lambda_0 = 632.8$ -nm line, or  $n = 1.348$  for the  $\lambda_0 = 351.1$ -nm line, was employed to calculate  $K^2 = (4\pi n/\lambda_0)^2 \sin^2(\theta/2)$ , where  $\theta$  is the scattering angle.

**Fluorescence Polarization Anisotropy (FPA) Measurements.** Time-resolved measurements of the fluorescence polarization anisotropy of ethidium dye intercalated in supercoiled pBR322 DNA with and without SSB protein bound were performed as described previously (Thomas et al., 1980a; Thomas & Schurr, 1983). The amount of added ethidium was small enough (less than 1 ethidium for every 200 base pairs) that unwinding of the helix by the dye was negligible compared to the native superhelical density of the plasmids. As we were interested in the properties of the equilibrium state, only samples that were 4–6 weeks old which had ceased to show time-dependent changes were used for the FPA (and for the light-scattering) experiments. In all measurements,  $T = 20 \pm 0.2$  °C.

The addition of 15 mol/mol of SSB protein resulted in the appearance of a fast component in the sum fluorescence with a lifetime in the range 0.5–0.8 ns. The slower component, which in all cases was more than 90% of the total fluorescence, had a lifetime of  $21.0 \pm 0.8$  ns which is indicative of a normal intercalation site for ethidium. A solution containing SSB protein and ethidium, but no DNA, exhibited a multicomponent fluorescence decay with lifetimes in the ranges 0.5–0.8 and 15–17 ns, which indicates that the ethidium does bind directly to free SSB protein. We tentatively assign the fast decaying component from solutions containing DNA, SSB protein, and ethidium to dye molecules attached to SSB proteins but cannot say whether the latter are bound or free.

The difference data  $d(t) = I_{||}(t) - I_{\perp}(t)$  were fit by using the intermediate zone formula (Allison & Schurr, 1982; Schurr, 1984) where  $I_{||}(t)$  and  $I_{\perp}(t)$  are the instantaneous emission intensities with polarizations parallel and perpendicular, respectively, to those of the exciting light pulse. For pBR322 with SSB protein, it was necessary to exclude the data at short times due to the fast component. The fit to the fluorescence data was started  $\sim 2$  ns after the end of the excitation pulse, which was operationally defined as the point where the excitation profile first falls to less than 0.5% of its peak height. The instrumental line width was approximately 550 ps. Satisfactory fits were obtained with reduced  $\chi^2$  values  $\leq 1.5$ .

The uniformity of  $\alpha$  was examined by performing FPA experiments over the intervals 0–18, 0–38, 0–76, and 0–120 ns, as also done previously (Thomas et al., 1980a; Thomas & Schurr, 1983).

**Fluorescence Titrations.** SSB protein shows a pronounced fluorescence quench upon binding to DNA (Krauss et al., 1981). This effect was utilized to measure the binding to supercoiled plasmid DNA independently. Titrations were performed in a Schoeffel RRS 1000 fluorometer as described by Krauss et al. (1981), by exciting the protein tryptophan fluorescence at 296 nm and monitoring the emission at 340 nm. The experiments were performed at 40 °C in 20 mM potassium phosphate, pH 7.4, and 50 mM NaCl.

Titration curves were collected by adding plasmid DNA to the SSB protein solution. The resultant fluorescence vs. added DNA titration curve was analyzed by means of a nonlinear least-squares fitting program (Peters & Pingoud, 1979). The quality of the fit was controlled by holding the number of

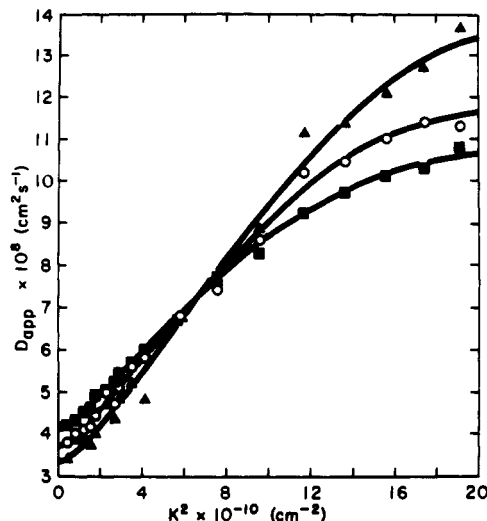


FIGURE 1: Apparent diffusion coefficient  $D_{app}$  vs.  $K^2$  ( $K^2$  is the square of the scattering vector) for supercoiled pBR322 DNA at 50  $\mu\text{g}/\text{mL}$ . (■) 0, (○) 3, and (▲) 10 mol of SSB protein was added per mole of DNA.

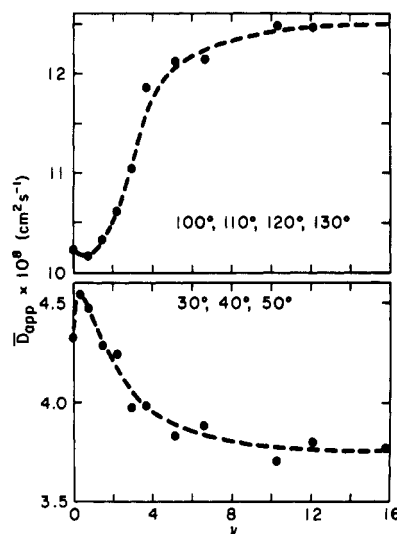


FIGURE 2: Average  $D_{app}$  values at low and high  $K^2$  for pBR322 DNA as a function of added SSB protein. The abscissa gives the stoichiometry of added SSB protein; ordinates are average  $D_{app}$  values at 30°, 40°, and 50° for  $\lambda = 632.8$  nm (lower panel) and at 100–130° for  $\lambda = 351.1$  nm (upper panel).

binding sites constant at different values while the other parameters (fluorescence of bound and free protein and the binding constant) were fitted by the program.

## RESULTS AND DISCUSSION

**Stoichiometry and Effect of Binding on DNA Conformation.** Figure 1 shows the  $D_{app}$  vs.  $K^2$  curves for pBR322 plasmid DNA in the presence of varying amounts of *E. coli* SSB protein. These data indicate that the apparent diffusion coefficient ( $D_{app}$ ) at low  $K^2$  decreases with increasing amounts of SSB protein. Since the extrapolated value of  $D_{app}$  at  $K^2 \rightarrow 0$  is the center of mass translational diffusion coefficient  $D_0$  of the molecule, the plasmid/protein complex evidently has a lower  $D_0$  than uncomplexed plasmid DNA. This decrease in  $D_0$  with added SSB protein is similar to an ethidium titration of the sedimentation coefficient of a superhelical DNA (Wang, 1969; Dean & Lebowitz, 1971), except that the curve does not pass beyond the minimum (Figure 2). Further, as  $D_0$  decreases, the plateau value of  $D_{app}$  at high  $K^2$  ( $D_{plat}$ ) increases,

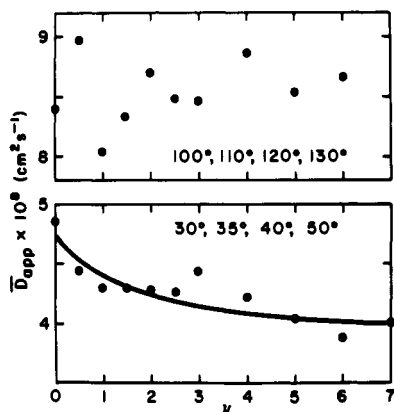


FIGURE 3: Average  $D_{app}$  values at low and high  $K^2$  for pUC8 DNA as a function of added SSB protein, analogous to Figure 2.

and both parameters actually seem to follow a hyperbolic binding curve with respect to the amount of SSB protein added.

Even with the UV light-scattering system, an actual plateau value could not be reached for  $D_{app}$ , so we averaged the  $D_{app}$  values at the four highest scattering angles, where  $D_{app}$  starts to level off (Figure 1). Similarly, an estimate for  $D_0$  was obtained by averaging the three  $D_{app}$  values at the lowest scattering angles for the red laser line. We considered this procedure legitimate, as we were only interested in relative changes of these quantities.

A slight sigmoidicity occurred in the  $D_0$  binding curve of pBR322, which was not observed in the pUC8 SSB protein experiments. Even though pUC8 follows the same qualitative behavior as pBR322 when SSB protein is bound (Figure 3), the increase in  $D_{plat}$  is barely detectable, if present at all.

The shape of the binding curve shown in Figures 2 and 3 as well as the available data on the binding of SSB protein to single-strand DNA (Krauss et al., 1981; Ruyechan & Wetmur, 1975) suggests that a clear-cut interpretation of the titration in terms of a binding constant and the number of binding sites is not feasible. First, the binding constant of a single SSB protein tetramer to a 40 base pair (bp) single-strand oligonucleotide is  $5 \times 10^8 \text{ M}^{-1}$  (Krauss et al., 1981), and the cooperative binding constant is  $10^{10}$ – $10^{11} \text{ M}^{-1}$  (Ruyechan & Wetmur, 1975). Since we employed DNA concentrations of 16.3–24.2 nM (in DNA molecules) or 71 (pBR322) and 66 (pUC8)  $\mu\text{M}$  in base pairs, and SSB protein concentrations of up to 258 nM, we are above the concentration range ( $c \approx K_{assoc}^{-1}$ ) in which accurate determinations of binding constants are possible by at least a factor of 10. The high cooperativity factor, of course, makes things even worse. We must therefore conclude that the curve only provides information about binding stoichiometry. Second, the titration curve for pBR322 clearly shows an initial increase in  $D_0$  prior to its drop at higher concentrations of SSB protein, indicating that a conformational transition other than a simple two-state process occurs. This observation makes a quantitative assignment of the amount of bound protein relative to the drop in  $D_0$  impossible. The quantity that can be reliably extracted from the binding curves is the stoichiometry. Since under the conditions employed here all of the protein is bound to the DNA, the approximate maximum binding stoichiometry is obtained from the point on the curve where  $D_0$  does not change with addition of more SSB protein. We find that the maximum binding stoichiometry for pBR322 is 8 mol of SSB tetramer per mole of DNA and for pUC8 4 mol/mol.

The observed 20% decrease in  $D_0$  when SSB protein binds to supercoiled DNA cannot be attributed simply to the larger

hydrodynamic friction of a nonspecific DNA/protein complex in which the DNA tertiary conformation is unaltered. The change in  $D_0$  caused by the binding of a globular protein like SSB protein to a supercoiled DNA of this size, if the shape of the DNA were not changed, would be much smaller than what we observe in pBR322. The argument is as follows. If we assume that all 10 SSB protein molecules bind to a single region on pBR322, then one short segment of DNA would be significantly increased in diameter. SSB protein has a molecular weight of 80000. Assuming a partial specific volume  $\bar{v} = 0.75 \text{ cm}^3/\text{g}$  gives a radius  $r = 2.9 \text{ nm}$  for each molecule. Ten SSB protein molecules engaged in nonspecific side by side binding without melting of the DNA would then occupy a length  $L = 58 \text{ nm}$  on the DNA. We now define a friction factor  $\tilde{f}$  per unit length for supercoiled pBR322 by simply dividing the total friction factor  $f = kT/D_0 = 9.9 \times 10^{-10} \text{ kg s}^{-1}$  by the contour length of the molecule  $L_c = 4363 \times 0.34 = 1483 \text{ nm}$  to obtain  $\tilde{f} = 6.68 \times 10^{-4} \text{ kg s}^{-1} \text{ m}^{-1}$ . Then, a 58-nm segment effectively contributes  $f_{sh} = (58 \times 10^{-9})\tilde{f} = 3.87 \times 10^{-11} \text{ kg s}^{-1}$  to the total friction. Were this segment moving freely as a rigid rod in solution, its friction factor would be (Tirado & Garcia de la Torre, 1979)

$$f_{seg} = 3\pi\eta \frac{L}{\ln(L/2r_h) + \gamma} = 1.57 \times 10^{-10} \text{ kg s}^{-1} \quad (1)$$

wherein  $\gamma$  is a function of  $L/2r_h$  and the hydrodynamic radius  $r_h = 1.25 \text{ nm}$  has been employed. This value is, of course, much larger than the friction contribution of the same segment within a longer supercoiled DNA molecule because of hydrodynamic shielding in the latter environment. However, we assume that the shielded friction factor of a 58-nm DNA segment in the larger DNA would increase upon protein binding by approximately the same factor as would the (unshielded) friction factor of the same segment free in solution. If 10 molecules of SSB protein bind to the 58-nm DNA segment, the geometry of the complex can be approximated by a new cylinder of the same length but radius  $r_{complex} = (r_{DNA}^2 + r_{protein}^2)^{1/2}$ . For the values given above,  $r_{complex} = 3.1 \text{ nm}$ , and the friction factor of the free complex is  $f_{complex} = 2.1 \times 10^{-10} \text{ kg s}^{-1}$ . This is an increase of 34% over the value for the free uncomplexed DNA segment. This means that the hydrodynamically shielded piece complexed with protein would now also contribute 34% more to the total friction, namely,  $1.34f_{sh} = 5.2 \times 10^{-11} \text{ kg s}^{-1}$ . Remaining uncomplexed DNA would contribute  $[(1483 - 58) \times 10^{-9}]\tilde{f} = 9.52 \times 10^{-10} \text{ kg s}^{-1}$ , making the total friction of the pBR322/SSB protein complex  $1.00 \times 10^{-9} \text{ kg s}^{-1}$ . This corresponds to an increase of only 1.4% over the value of free pBR322, which is much less than was actually observed. Binding of all the SSB protein molecules to one region on the DNA without changing its conformation therefore cannot account for our observations.

Another possibility that can also be excluded is that the protein distributes itself more or less homogeneously along the DNA chain. With the volume of the DNA being  $1483\pi r_{DNA}^2 = 7280 \text{ nm}^3$  and a total volume of 10 SSB protein molecules of  $996 \text{ nm}^3$ , the total volume of the new chain would be  $8276 \text{ nm}^3$ , giving an average radius (with the contour length remaining constant) of 1.33 nm. When eq 1 is employed, the increase in the friction factor for a 1483-nm cylinder with the radius increasing from 1.25 to 1.33 nm is 1% and therefore cannot explain our data. Thus, we can conclude that the change in  $D_0$  which occurs upon binding of the SSB protein must be due to an alternation of the conformation of the superhelical DNA.

Supercoiled DNA has been reported to contain sites sensitive to single-strand-specific nucleases (Lilley, 1980; Panayotatos

& Wells, 1981; Goding & Russell, 1983; Glikin et al., 1983). Furthermore, observations from electron microscopy combined with S1 digestion data (Glikin et al., 1983) suggest that *E. coli* SSB protein binds to these as well as other sites on the DNA. Although the DNA studied in the latter reference was not pBR322, this DNA also possesses single-strand nuclease-sensitive sites (Lilley, 1980). Therefore, the most straightforward explanation for the observed behavior of  $D_0$  is that *E. coli* SSB protein interacts with supercoiled DNA by binding to one or more regions with latent single-strand character, melting the double helix, and thereby through removal of superhelical turns altering the global conformation of the DNA. The overall shape of the titration curve, namely, an initial increase and a later decrease in  $D_0$ , is reminiscent of titrations of superhelical DNA with ethidium (Upholt et al., 1971; Dean & Lebowitz, 1971; Wang, 1974) in which an initial increase of the  $s$  value at low ethidium binding densities is seen which is then followed by a decrease as binding of more ethidium relaxes the DNA completely. We conclude in analogy to the results of the ethidium titrations reported by Upholt et al. (1971) that the hydrodynamic behavior of the pBR322/SSB complex is mainly determined by the superhelical density of the DNA.

The stoichiometry that we observe is in agreement with this interpretation. As shown in Figure 2, the increase in  $D_0$  corresponding to the initial conformational alteration occurs at ca. two SSB protein tetramers, and the drop in  $D_0$  is complete at a stoichiometry of approximately eight SSB protein tetramers per pBR322 molecule. Each molecule of SSB protein covers 65 nucleotides of DNA (T. Lohman, personal communication). Assuming 10.5 base pairs per turn, 8 SSB proteins will therefore unwind 25 helix turns. The native superhelical density of plasmids like pBR322 (Bauer, 1978) is  $-0.05$  to  $-0.07$ , so with 415 helix turns, it has approximately 20–30 negative superhelical turns. We conclude that binding of SSB protein proceeds until nearly all of the superhelical turns are removed. pUC8 is saturated at approximately four SSB tetramers per DNA (Figure 3). This plasmid contains 2717 base pairs and, assuming the same superhelical density, should have 13–18 superhelical turns. The binding of SSB proteins removes  $130/10.5 = 12.4$  superhelical turns. Here, too, SSB protein binds up to a point where nearly all of the native superhelical turns are relaxed.

**Fluorescence Titrations.** In order to get an independent measurement of the binding stoichiometry of SSB protein to pBR322, the binding protein was titrated with superhelical pBR322 DNA in a fluorometric experiment. The resulting binding curve is shown in Figure 4. The titration was fitted by a nonlinear fitting routine as described under Materials and Methods. The best fit (theoretical curve in Figure 4) was obtained with  $n = 10$  independent binding sites and a binding constant  $K_{\text{assoc}} = 2.6 \times 10^7 \text{ M}^{-1}$ , although  $n = 8$  binding sites and  $K_{\text{assoc}} = 5.7 \times 10^7 \text{ M}^{-1}$  yields a theoretical curve that is nearly indistinguishable.

These stoichiometries are in very good agreement with the approximate values from our light-scattering data. The fact that a good fit to the fluorescence data was obtained with a model that employed independent binding sites seems to indicate that the binding cooperatively is not very high in this case. However, it may also reflect a decline in the binding constant with loss of superhelical turns, which is a kind of anticooperativity that should significantly offset the effects of otherwise cooperative binding.

**Gel Electrophoresis.** The dissociation kinetics of SSB protein from supercoiled DNA can be estimated from the

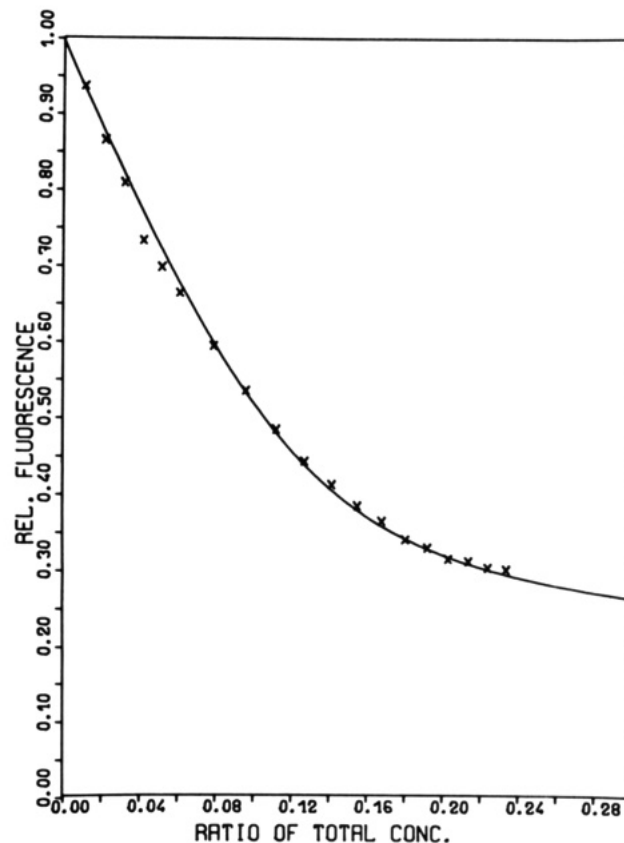


FIGURE 4: Fluorescence titration of 86 nM SSB protein solution with 128 nM pBR322 solution. Buffer: 0.02 M potassium phosphate, pH 7.4, and 0.05 M NaCl.

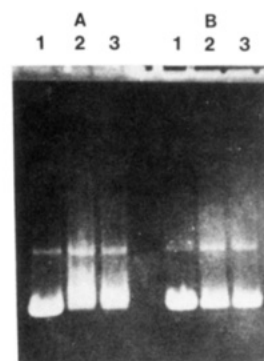


FIGURE 5: Agarose gel electrophoresis of pUC8 DNA without (lane 1) and with (lanes 2 and 3) 10 mol/mol of SSB protein added. (A) Samples without sodium dodecyl sulfate (SDS); (B) samples with 0.1% SDS added. Electrophoresis was in a 1% agarose gel containing 40 mM Tris, 5 mM boric acid, and 1 mM  $\text{Na}_2\text{EDTA}$  at pH 8.5 for 6 h at 3.5 V/cm. Center of band migration distances were 73 mm for uncomplexed pUC8, 70 mm for complexed pUC8, and 56 mm for open circular pUC8.

behavior of the complex in agarose gel electrophoresis. Figure 5 shows that the DNA complexed with SSB protein runs slower than the free DNA, probably due to the altered tertiary conformation of the DNA in the complex. If one adds 0.1% sodium dodecyl sulfate (SDS) to the gel sample before loading the gel, the DNA (lanes labeled B) runs in the same place as the control free DNA. The band of the SSB protein complexed DNA is blurred, which indicates that some or all of the protein has dissociated within the 3 h of electrophoresis. However, the dissociation must be slow enough to retard the band.

If we assume the relaxed SSB protein/DNA complex runs with approximately the same mobility as open circular DNA

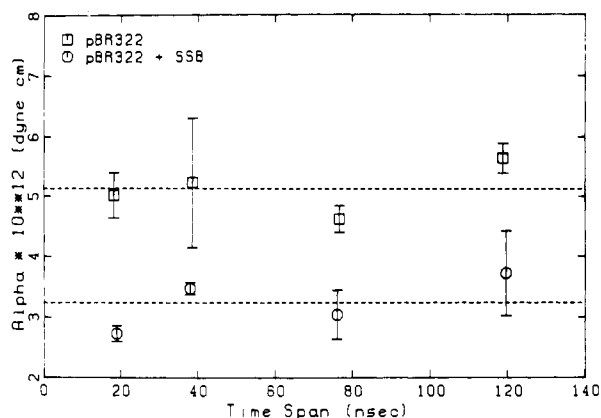


FIGURE 6: Torsion constant of free and SSB protein complexed pBR322 DNA as measured in an FPA experiment. Buffer: 0.01 M sodium cacodylate, pH 7.2, 1 mM EDTA, and either 0.01 M NaCl (upper curve) or 0.1 M NaCl (lower curve).

and assign a dissociation time before which all the SSB protein is bound and after which all of it is free, the partially relaxed SSB protein bound DNA band will run at a position between the supercoiled and open circular bands which is determined by the ratio of the dissociation time to the total time of electrophoresis. Since in our particular experiment in Figure 5 the open circular DNA lags 17 mm behind the supercoil and the SSB protein/DNA complex lags 3 mm, the dissociation time would be approximately 1 h if the total electrophoresis time was 6 h. Even though this estimate is only a very crude approximation, we may say that the dissociation rate constant of SSB protein from supercoiled pBR322 DNA should be in the range of  $10^{-2}$ – $10^{-3}$  s<sup>-1</sup>. This dissociation rate is in approximate agreement with values reported by Krauss et al. (1981). Evidently, none of the DNA from solutions containing 15 mol/mol of SSB protein migrates as fast as the free DNA. It may be inferred that the distribution of SSB protein among the DNA molecules under these saturation binding conditions is not so uneven that a significant fraction of the DNA has no bound SSB protein.

**Effect of Binding on Internal Dynamics.** We now focus on the high  $K^2$  region of the scattering curve, which reflects the dynamics of internal motions. The plateau value  $D_{\text{plat}}$  of the apparent diffusion coefficient at large  $K^2$  either increases substantially (pBR322) or remains unchanged (pUC8), whereas  $D_0$  decreases in both cases upon binding SSB protein. Thus, the mobility of local segments of the DNA relative to the center of mass, which is reflected in the difference  $D_{\text{plat}} - D_0$ , is evidently increased as the supercoils are removed. Our tentative interpretation of this change is that self-entanglement in the (presumed) interwound supercoiled DNA restricts the amplitudes of many interval motions but in the relaxed circular form such restrictions are largely removed and greater amplitudes of subunit motion prevail.

**FPA Measurements (Torsional Rigidity).** After addition of 15 mol/mol of SSB protein, the apparent torsion constant ( $\alpha$ ) of pBR322 decreases from  $5.2 \times 10^{-12}$  to  $3.2 \times 10^{-12}$  dyn cm (Figure 6). This marked decrease in the torsion constant is very similar to the reduction in  $\alpha$  observed initially following linearization of pBR322 by *EcoRI* (unpublished results). A similar drop in  $\alpha$  was reported by Shibata et al. (1984) for linearized M13mp7 DNA and has also been observed for linearized pUC8 DNA (unpublished results). In the case of the linearized plasmids, after the initial drop,  $\alpha$  actually rises over a period of  $\sim 8$  weeks, sometimes passing through a maximum before approaching the equilibrium value for the linearized form. A tentative explanation of such phenomena

is given elsewhere (Shibata et al., 1984). In any case, we did not follow the time evolution of  $\alpha$  for the pBR322/SSB protein complex.

The constancy of  $\alpha$  with the time span of the experiment, as shown in Figure 6, indicates that the torsional rigidity is uniform in the sense that major rigidity weaknesses do not occur in the range from 1 per 20 bp to about 1 per 1000 bp. That is, uninterrupted segments of duplex DNA are about 1000 bp or longer, even in the SSB/pBR322 complex.

#### ACKNOWLEDGMENTS

We thank Louise Rose for her expert illustration work.

#### REFERENCES

- Allison, S. A., & Schurr, J. M. (1978) *Chem. Phys.* 41, 35.  
 Bauer, W. (1978) *Annu. Rev. Biophys. Bioeng.* 7, 287.  
 Dean, W. W., & Lebowitz, J. (1971) *Nature (London), New Biol.* 231, 5.  
 Glikin, G. C., Gargiulo, G., Rena-Descalzi, L., & Worcel, A. (1983) *Nature (London)* 303, 770.  
 Goding, C. R., & Russell, W. C. (1983) *Nucleic Acids Res.* 11, 21.  
 Jovin, T. M., McIntosh, L. P., Arndt-Jovin, D. J., Zarling, D. A., Robert-Nicoud, M., van de Sande, J. H., Jorgenson, K. F., & Eckstein, F. (1983) *J. Biomol. Struct. Dyn.* 1, 21.  
 Krauss, G., Sindermann, H., Schomburg, U., & Maass, G. (1981) *Biochemistry* 20, 5346.  
 Langowski, J., Fujimoto, B. S., Wemmer, D., Benight, A. S., Drobny, G., Shibata, J. H., & Schurr, J. M. (1984) *Biopolymers* (in press).  
 Lilley, D. M. J. (1980) *Proc. Natl. Acad. Sci. U.S.A.* 77, 6468.  
 Lilley, D. M. J., & Markham, A. F. (1983) *EMBO J.* 2, 527.  
 Lin, S.-C. & Schurr, J. M. (1978) *Biopolymers* 17, 425.  
 Lin, S.-C., Thomas, J. C., Allison, S. A., & Schurr, J. M. (1981) *Biopolymers* 20, 209.  
 Maniatis, T., Fritsch, E. F., & Sambrook, J. (1982) in *Molecular Cloning*, p 68, Cold Spring Harbor Laboratory, Cold Spring Harbor, NY.  
 Mizuuchi, K., Mizuuchi, M., & Gellert, M. (1982) *J. Mol. Biol.* 156, 229.  
 O'Connor, T., Kilpatrick, M. W., Klysik, J., Larson, J. E., Martin, J. C., Singleton, C. K., Stirdivant, S. M., Zacharias, W., & Wells, R. D. (1983) *J. Biomol. Struct. Dyn.* 1, 999.  
 Panayotatos, N., & Wells, R. D. (1981) *Nature (London)* 289, 466.  
 Peters, F., & Pingoud, A. M. (1979) *Int. J. Bio-Med. Comput.* 10, 401.  
 Pohl, F., & Jovin, T. M. (1972) *J. Mol. Biol.* 67, 375.  
 Rouse, P. E. (1953) *J. Chem. Phys.* 21, 1272.  
 Ruyechan, W. T., & Wetmur, G. (1975) *Biochemistry* 14, 5529.  
 Schurr, J. M. (1977) *CRC Crit. Rev. Biochem.* 4, 371.  
 Schurr, J. M. (1984) *Chem. Phys.* 84, 71.  
 Shibata, J. H., Wilcoxon, J., Schurr, J. M., & Knauf, V. (1984) *Biochemistry* 23, 1188.  
 Thomas, J. C., & Schurr, J. M. (1983) *Biochemistry* 22, 6194.  
 Thomas, J. C., Allison, S. A., Appellof, C. J., & Schurr, J. M. (1980a) *Biophys. Chem.* 12, 177.  
 Thomas, J. C., Allison, S. A., Schurr, J. M., & Holder, R. D. (1980b) *Biopolymers* 19, 1451.  
 Tirado, M. M., & Garcia de la Torre, J. (1979) *J. Chem. Phys.* 71, 2581.  
 Upholt, W. B., Gray, H. B., & Vinograd, J. (1971) *J. Mol. Biol.* 62, 21.  
 Wang, A. H.-J., Quigley, G. J., (1979) Kolpak, F. J., Crawford, J. L., van Boom, J. H., van der Marel, G., & Rich,

A. (1979) *Nature (London)* 282, 680.  
 Wang, J. C. (1969) *J. Mol. Biol.* 43, 25.  
 Wang, J. C. (1974) *J. Mol. Biol.* 87, 797.  
 Wilcoxon, J. (1983) Ph.D. Thesis, University of Washington, Seattle, WA.

Wilcoxon, J., Shibata, J. H., Thomas, J. C., & Schurr, J. M. (1982) in *Biomedical Applications of Laser Light Scattering* (Sattelle, D. B., Lee, W. I., & Ware, B. R., Eds.) pp 21-36, Elsevier, Amsterdam.  
 Zimm, B. H. (1956) *J. Chem. Phys.* 24, 269.

## Characteristics of the Binding of the Anticancer Agents Mitoxantrone and Ametantrone and Related Structures to Deoxyribonucleic Acids<sup>†</sup>

J. William Lown,\*<sup>‡</sup> A. Richard Morgan,<sup>§</sup> Shau-Fong Yen,<sup>||</sup> Yueh-Hwa Wang,<sup>||</sup> and W. David Wilson<sup>||</sup>

*Departments of Chemistry and Biochemistry, University of Alberta, Edmonton, Alberta T6G 2G2, Canada, and Department of Chemistry, Georgia State University, Atlanta, Georgia 30303*

*Received October 28, 1984*

**ABSTRACT:** The binding constants for interaction of the anticancer agents mitoxantrone and ametantrone and several congeners with calf thymus DNA and the effects of ionic strength changes have been determined spectrophotometrically. The agents show a preference for certain sequences, particularly those with GC base pairs, and the magnitude of the specificity depends on the specific substituents on the anthraquinone ring system. The binding constant for mitoxantrone with calf thymus DNA in 0.1 M Na<sup>+</sup>, pH 7, is approximately  $6 \times 10^6 \text{ M}^{-1}$ , and the rate constant for the sodium dodecyl sulfate driven dissociation of mitoxantrone from its calf thymus DNA complex under the same solution conditions and 20 °C was determined to be  $1.3 \text{ s}^{-1}$ . The unwinding angle of mitoxantrone determined independently by viscosity measurements and by a novel assay employing calf thymus topoisomerase shows excellent agreement for a value of 17.5°. The viscosity increase of sonicated calf thymus DNA varies considerably with the substituent on the anthraquinone ring system. Binding studies employing T4 and  $\phi$ w-14 DNAs in which the major groove is occluded and the reverse experiment with anthramycin-treated calf thymus DNA indicate at least part of the mitoxantrone molecule may lie in the minor groove.

**A**lthough doxorubicin (adriamycin) shows wide-spectrum activity against a range of human malignancies (Arcamone, 1978, 1981), its clinical efficacy is currently limited by the severe risk of irreversible cardiac damage (Bonadonna, Monfardini, 1969; Lenaz et al., 1976; Smith, 1969). Consequently intensive efforts have been undertaken both to understand the underlying molecular origin of the cardiotoxicity (Doroshov et al., 1980; Lown et al., 1982; Goodman & Hochstein, 1977) and thereby to obviate or minimize it by structural modification (Tong et al., 1979) or by the rational design and de novo synthesis of less toxic drugs (Lown et al., 1981). Among the more promising drugs developed are the anthracene derivatives 1,4-dihydroxy-5,8-bis[[2-[(2-hydroxyethyl)amino]ethyl]amino]-9,10-anthracenedione [mitoxantrone (1); Figure 1] and its congeners (Murdock et al., 1979).

Biochemical evidence suggests that, in common with the anthracyclines, nucleic acids are among the principal cell targets of these drugs and that they cause inter alia profound changes in chromatin structure including compaction (Traganos et al., 1980; Waldes & Center, 1982; Bowden et al., 1982; Citarella et al., 1982). Although the experience with

other clinically useful anticancer drugs would suggest parallel modes of action involving other cellular macromolecules (Lown, 1983), there are strong indications that interaction of mitoxantrone with cellular DNA contributes significantly to the cytotoxic action. However, the exact nature of the DNA interactions is at present unclear. We recently reported electron microscopy evidence for the intercalative binding of mitoxantrone and bis[(4,5-dihydro-1H-imidazol-2-yl)-hydrazone] 9,10-anthracenedicarboxaldehyde (bisantrene) to different DNAs and the phenomenon of inter-DNA interactions and association produced by mitoxantrone and certain congeners (Lown et al., 1984). Since the unique shape of these drugs apparently prevents intercalation of all parts of the chromophore in contrast to doxorubicin (Neidle, 1978), we report an examination of the substituent dependence in the binding of mitoxantrone and its congeners to DNA. In addition, we report the measurement of their binding constants to DNA and the kinetics of dissociation together with a determination of the unwinding angle by two independent methods and a determination of the groove and base preference for DNA binding in order to characterize the DNA binding of this important class of anticancer agents.

### MATERIALS AND METHODS

#### Materials

**Compounds.** Mitoxantrone, ametantrone, and their congeners (1-9) (Figure 1) were supplied by Dr. K. C. Murdock of Lederle Laboratories, Pearl River, NY. Their synthesis, purification, and properties have been described previously (Murdock et al., 1979). Daunorubicin was purchased from

<sup>†</sup>This investigation was supported by grants (to J.W.L.) from the National Cancer Institute of Canada and the Natural Sciences and Engineering Council of Canada, a contract with the National Foundation for Cancer Research, a grant (to A.R.M.) from the Medical Research of Canada, and a grant (to W.D.W.) from the National Institutes of Health (GM30267).

\*Department of Chemistry, University of Alberta.

†Department of Biochemistry, University of Alberta.

||Department of Chemistry, Georgia State University.